Compound sophorae decoction enhances intestinal barrier function of dextran sodium sulfate induced colitis via regulating notch signaling pathway in mice

Hui Wu[1], Qian-Yun Chen[1], Wen-Zhu Wang[1], Si Chu, Xing-Xing Liu, Yu-Jin Liu, Chen Tan, Feng Zhu, Shuang-Jiao Deng, Ya-Lan Dong, Ting Yu, Fei Gao, Hong-Xia He, Xue-Yuan Leng, Heng Fan*

Department of Integrated Traditional Chinese and Western Medicine, Union Hospital, Tongji Medical College, Huazhong University of Science and Technology, Wuhan, 430022, China

ARTICLEINFO

Keywords:
Ulcerative colitis
Compound sophorae decoction
Barrier function
Intestinal epithelial cells
Mucus
Notch

ABSTRACT

Background: Compound sophorae decoction (CSD), a Chinese Herbal decoction, is frequently clinically prescribed for patients suffered from ulcerative colitis (UC) characterized by bloody diarrhea. Yet, the underlying mechanism about how this formulae works is remain elusive.

Methods: In the present study, the experimental colitis in C57BL/6 J mice was induced by oral administration of standard diets containing 3% dextran sodium sulfate (DSS), and CSD was given orally for treatment at the same time. The clinical symptoms including stool and body weight were recorded each day, and colon length and its histopathological changes were observed. Apoptosis of colonic epithelium was studied by detecting protein expression of cleaved caspase-3, and cell proliferation by Ki-67 immunohistochemistry. Tight junction complex like ZO-1 and occludin were also determined by transmission electron microscope and immunofluorescence. The concentration of FITC-dextran 4000 was measured to evaluate intestinal barrier permeability and possible signaling pathway was investigated. Mucin2 (MUC2) and notch pathway were tested through western blot. The M1/M2 ratio in spleen and mesenteric lymph nodes were detected by flow cytometry. And the mRNA levels of iNOS and Arg1 were examined by qRT-PCR.

Results: CSD could significantly alleviate the clinical manifestations and pathological damage. Body weight loss and DAI score of mice with colitis were improved and shortening of colon was inhibited. The administration of CSD was able to reduce apoptotic epithelial cells and facilitate epithelial cell regeneration. Increased intestinal permeability was reduced in DSS-induced colitis mice. In addition, CSD treatment obviously up-regulated the expression of ZO-1 and occludin and the secretion of MUC2, regulated notch signaling, and decreased the ratio of M1/M2.

Conclusions: These data together suggest that CSD can effectively mitigate intestinal inflammation, promote phenotypic change in macrophage phenotype and enhance colonic mucosal barrier function by, at least in part, regulating notch signaling in mice affected by DSS-induced colitis.

1. Introduction

Ulcerative colitis, an idiopathic and chronic inflammatory disease, affects the colon and rectum confined to mucosa and submucosa. Bloody diarrhea and abdominal pain are the main clinical presentation. Though the pathogenesis of UC continues to elude researchers, environmental factors, genetic predisposition, dysregulated immune responses and mucous barrier and epithelial barrier defects are believed to be strongly implicated in the pathophysiology of UC. Despite the fact that medical management including 5-ASA (5-aminosalicylic acid) drugs, corticosteroids, immunosuppressants and biological preparations has been developed to induce and maintain remission, there is no cure for this relapsing and remitting intestinal inflammation. Hence, it is necessary to find more effective treatments. It has been reported that traditional Chinese medicine prescriptions like herbal medicine [1] and acupuncture [2] contribute to improve symptoms and relieve inflammation in patients with UC.

Compound sophorae decoction is composed of six Chinese herbs including Sophora flavescens Ait., Sanguisorba officinalis L. (carbonizing by stir-frying), Bletilla striata (Thunb.) Reichb.f., Glycyrrhiza uralensis Fisch., Baphicacanthus cusia (Nees) Bremek and panax notoginseng (Burk.) F.H.Chen. at the proportion of is 15:15: 10:10: 3:3. Our previous experimental data has demonstrated that this agent could relieve inflammatory response and regulate the immune function by influencing Th17/Treg cell balance in mice with UC [3] and execute the ulcerative colitis-related colorectal cancer (UCRCC)-inhibitory activity [4]. In several years of clinic practice, CSD, which can heat-clearing, detoxification and dryness, has been proven to be beneficial in the treatment of mild-to-moderate active UC characterized by dampness and heat

* Corresponding author at: 1277 Jiefang Avenue, Jianghan District, Wuhan 430022, Hubei, China.
E-mail address: fanheng009@aliyun.com (H. Fan).
[1] These authors have contributed equally to this work.

https://doi.org/10.1016/j.biopha.2020.110937
Received 3 May 2020; Received in revised form 18 October 2020; Accepted 25 October 2020
Available online 17 November 2020
0753-3322/© 2020 Published by Elsevier Masson SAS. This is an open access article under the CC BY-NC-ND license (http://creativecommons.org/licenses/by-nc-nd/4.0/).

accumulation in light of the traditional Chinese medical theory.

A growing number of studies have shown that defects in enterocyte and mucus layer composition will lead to compromised gut barrier function causing increased intestinal permeability coupled with elevated exposition to luminal content and excessive immune reaction that would promote intestinal inflammation [5]. On account of this, we hypothesized that if the therapeutic effect of CSD on relieving the symptoms such as abdominal pain and bloody diarrhea is related to its possible role in restoring intestinal barrier function. Therefore, to clarify the efficacy and potential mechanisms of CSD in mice with DSS-induced colitis, we analyzed molecules or cells involved in alterations in intestinal barrier function.

2. Materials and methods

2.1. Animals

Male C57BL/6 J mice (7–8 weeks old, weighting 21− 25 g) were purchased from SPF (Beijing) Biotechnology Co.,Ltd. (Quality Certification of Laboratory Animals: SCXK (jing) 2019− 0010). During the experiment, mice were housed in a specific pathogen-free environment of 12 h dark/light cycles, room temperature 22–24 °C, and relatively constant humidity in the experimental animal center of Huazhong University of Science and Technology (HUST, Wuhan, China) (Permit number: SYXK(e)2016− 0057). And these animals were allowed to have access to food and water ad arbitrium. In this study, experimental procedures and animal care were conducted in strict accordance with the Animal Research Institute Committee guidelines of HUST, and approved by the Institutional Animal Care and Use Committee of HUST. *2.2. Preparation of compound sophorae decoction aqueous extract*

Compound sophorae decoction is composed of Sophora flavescens Ait., Sanguisorba officinalis L., (carbonizing by stir-frying), Bletilla striata (Thunb.) Reichb.f., Glycyrrhiza uralensis Fisch., Baphicacanthus cusia (Nees) Bremek and panax notoginseng (Burk.) F.H.Chen., which were obtained from Wuhan Union Hospital (Wuhan, China) and the batch numbers were 180401, 180401, 170701, 180301, 17,080,197 and 170801, respectively. The crude drugs were identified by Professor Xueyun Duan from Department of Pharmacy, Hubei Provincial Hospital of Traditional Chinese Medicine (Wuhan, China). All voucher specimens are deposited in the Laboratory of Integrated Tradition Chinese and Western Medicine, Union Hospital, Tongji Medical College, Huazhong University of Science and Technology (Wuhan, China) with numbers 2019041001, 2019041002, 2019041003, 2019041004, 2019041005 and 2019041006. Raw herbs were mixed in a ratio of 15:15:10:10:3:3 as shown in Table 1. Herbs except panax notoginseng (Burk.) F. H. Chen were decocted with distilled water twice, for 30 min each, and then the decoctions were filtered and pooled. After that, panax notoginseng (Burk.) F.H.Chen was added to the filtrate. Because the volume required for gavage in mice is usually small, the pooled solution was need to be further concentrated. The final concentration of CSD is 1.1648 g/mL (calculating with raw herbs). For the purpose of analysis by high- performance liquid chromatography-tandem mass spectrometric (HPLC-MS/MS), all herbal materials including panax notoginseng (Burk.) F. H. Chen were decocted in a process mentioned above with ultimate density of 1.0 g/mL.

Table 1
Components of CSD.

Chinese Name	Latin Name	Parts used in medicine	Proportion	efficacy
Ku shen	Sophora flavescens Ait	Root	15	Clearing heat; dryness
Di yu tan	Sanguisorba officinalis L.	Root	15	Hemostasis
Bai ji	Bletilla striata (Thunb.) Reichb. f.	Tuber	10	Astringency and hemostasis; dispersing swelling and promote tissue regeneration
Gan cao	Glycyrrhiza uralensis Fisch	Root and rhizome	10	Clearing heat; detoxifying; relieving spasm and pain
Qing dai	Baphicacanthus cusia (Nees) Bremek.	Leaf and stem leaf	3	Clearing heat; detoxifying
San qi	Panax notoginseng (Burk.) F. H. Chen	Root	3	Dispersing blood stasis and stop bleeding; promoting blood circulation and stopping pain

2.3. HPLC-MS/MS analysis

The decoctions were settled overnight at 4 °C and the supernatant was collected. The volume of 200 μL was accurately taken and added to 1 mL mixture of methanol and water (8:2, v/v), blended by vortex, and then subjected to centrifuge at 20,000 *g* for 10 min at 4 °C. The supernatant was filtered through a 0.22 μm filter before HPLC-MS/MS analysis. In addition, standards (Table 2) were accurately weighed, mixed, and dissolved in methanol to prepare a mixed standard solution of 10 μg/mL. The chemical analysis of extracts was carried out on a HPLC system of UltiMate 3000 RS (Thermo Scientific, Karlsruhe, Germany) and separation of the analytes was performed with Q Exactive high resolution mass spectrometer (Thermo Scientific, Karlsruhe, Germany).

Table 2
Standards.

Ingredients	Molecular formula	Molecular weight	Herb source
Matrine	C15H24N2O	248.36	Sophora flavescens Ait
Oxymatrine	C15H24N2O2	264.36	Sophora flavescens Ait
Gallic acid	C7H6O5	170.02	Sanguisorba officinalis L.
Liquiritin	C21H22O9	418.39	Glycyrrhiza uralensis Fisch
Glycyrrhizic acid	C42H62O16	822.93	Glycyrrhiza uralensis

			Fisch
Ginsenoside Rb1	C64H92O23	1109.29	Panax notoginseng (Burk.) F. H. Chen
Notoginsenoside R1	C47H80O18	933.13	Panax notoginseng (Burk.) F. H. Chen
Indigo	C16H10N2O2	262.26	Baphicacanthus cusia (Nees) Bremek.
Indirubin	C16H10N2O2	262.26	Baphicacanthus cusia (Nees) Bremek.

Standard references: Matrine (CAS:519-02-8), Oxymatrine (CAS:16837- 52-8), Gallic acid (CAS:149-91-7), Glycyrrhizic acid (CAS:1405-86-3), Ginsenoside Rb1 (CAS:41753-43-9), Notoginsenoside R1 (CAS:80418- 24-2) and Indirubin (CAS:479-41-4) were purchased from Aladdin Bio- Chem Technology (Shanghai, China); Liquiritin (CAS:551-15-5) and Indigo (CAS:482-89-3) were purchased from the National Institutes for Food and Drug Control (China).

2.4. Thin-layer chromatography (TLC) analysis

5 μL of each sample including CSD aqueous extracts, positive samples of Bletilla striata (Thunb.) Reichb. f. and negative controls was spotted on silica gel G plate and the system of cyclohexane/ethyl acetate/ methanol (6:2.5:1) was used as the development reagent and 10 % sulfuric acid ethanol solution as colorimetric method. Results were recorded under UV light (365 nm).

2.5. Construction of animal model and treatment

Mice were randomly divided into six groups (n = 10), that is, normal control (CON), model (DSS), CSD low dose (CSD-L, 3.64 g/kg), CSD medium dose (CSD-M, 7.28 g/kg), CSD high dose (CSD-H, 14.56 g/kg), and mesalazine SR Granules (mesalazine, 0.52 g/kg, Ipsen, Boulogne- Billancourt, France). Except the CON group, other mice were administered 3% (w/v) DSS (MW 36-50 kDa, Cat# 0216011080, MP Biomedicals, Illkirch, France) in drinking water for 7 consecutive days to induce acute colitis in mice. And mice were given corresponding therapeutic drugs once daily by gavage for 7 days, synchronizing the procedure of DSS induction. The CON group and the DSS group were administered the same amount of drinking water orally.

2.6. Assessment of severity of colitis

During the experiment, the body weight, stool consistency and presence of hemafecia of each mice were recorded daily. Disease activity index (DAI) of colitis was defined. The colorectal of the mice were harvested and the damage of intestinal mucosa was quantified by HE staining with histological score [6].

2.7. Quantitative real-time polymerase chain reaction (qRT-PCR)

Total RNA from colonic tissues was isolated with TRIzol (TaKaRa, Dalian, China). And reverse transcription was performed with PrimeScript™ RT Master Mix (TaKaRa, Dalian, China) to obtain complementary DNAs (cDNAs). Whereafter, cDNA fragments were amplified and analyzed to confirm genes expression changes using the SYBR Premix Ex TaqTM (TaKaRa, Dalian, China). mRNA levels of different samples were normalized to those of β-actin which are often referred to as housekeeping genes. Primer sequences are listed in Table 3.

2.8. Western blot

Protein was extracted by RIPA lysis buffer (Servicebio Technology, Wuhan, China) with a cocktail of protease inhibitions (Servicebio Technology, Wuhan, China) and the concentration of protein was detected by the BCA protein assay kit (Beyotime Biotechnology). 30 μg of total protein was separated on 10 % SDS-polyacrylamide gel electrophoresis (SDS-PAGE) and then transferred onto 0.45 μm Polyvinylidene fluoride (PVDF) membranes (Millipore, MA, USA). After being blocked with 5% skimmed milk, the membranes were incubated with primary antibodies at 4 °C overnight and then with secondary antibodies for 1 h at room temperature. Finally, the membranes were visualized by enhanced chemiluminescence (ECL) reagent (Millipore, MA, USA). The primary antibodies and its dilution concentration were as follows: cleaved caspase-3 (1:1000, ab2302, abcam, Cambridge, MA, USA), MMP-9 (1:500, ab38898, abcam), MUC2 (1:500, NB120-11197, Novus Biologicals, Littleton, Colorado, USA), ATOH1 (1:1000, 21215- 1-AP, proteintech), HES1 (1:1000, ab108937, abcam), Notch1 (1:1000, #3608, CST, Beverly, MA, USA) and β-Actin (1:10000, ab37168, abcam).

2.9. Immunohistochemistry and immunofluorescence staining

Immunohistochemistry [7] and immunofluorescence staining [8] were performed as previously described with some modification. Briefly, 5-μm-thick paraffin-embedded sections of colon tissue samples were deparaffinized by xylene and dehydrated by different concentration of alcohol solutions and then were treated with citrate buffer for antigen retrieval. 3 % H_2O_2 was used to block endogenous peroxidase for 15 min, followed by diluted goat serum to reduce nonspecific staining for 30 min. After that, the sections were incubated with primary antibody rabbit anti-Ki67 (1:200, ab16667, abcam, Cambridge, MA) at 4 °C overnight. Washed the slides three times with PBS, and added horseradish peroxidase (HRP) labeled goat anti-rabbit secondary antibody for 30 min. The sections were developed using 3,3-diaminobenzidine tetrahydrochloride (DAB) and contrasted using hematoxylin. Images were acquired using a light microscope. For immunofluorescence staining, ZO-1 (1:300, 21773-1-AP, proteintech) and occludin (1:200, 66378-1-Ig, proteintech) were used as primary antibodies and fluorescence labeled secondary antibody. A laser confocal scanning microscope (Olympus-FV1000, Tokyo, Japan) was applied.

2.10. Intestinal permeability analysis

Intestinal permeability was evaluated with fluorescein isothiocyanate (FITC)-Dextran 4000 (4

KDa, Cat# FD4, Sigma-Aldrich, St. Louis, MO, USA) test, as described previously [9]. Briefly, mice were fasted for 4 h and then FITC-dextran 4000 (600 mg/kg body wt) was administered by gavage. Four hours after gavage, whole blood was collected, and serum was isolated. The analysis for the fluorescence intensity of FITC-dextran 4000 in plasm was carried out with a multimode plate reader (PerkinElmer EnSpire Plate Reader, Waltham, MA, USA) (excitation, 490 nm; emission, 520 nm). Standard curves for calculating the FITC-dextran concentration were obtained by diluting FITC-dextran in PBS.

Table 3
Primer sequences for qRT-PCR.

Gene		Primer Sequences (5′–3′)	Length (bp)
β-actin	sense	CTGAGAGGGAAATCGTGCGT	208
	antisense	CCACAGGATTCCATACCCAAGA	
iNOS	sense	CATTCAGATCCCGAAACGCT	316
	antisense	TGTAGGACAATCCACAACTCGC	
TNF-α	sense	TCCCCAAAGGGATGAGAAGTT	298
	antisense	GAGGAGGTTGACTTTCTCCTGG	
MCP-1	sense	CCCTACTATTCCTGATGGCACT	159
	antisense	CTATGAGAAACCCACCACATCTG	
IL-1β	sense	GGGCCTCAAAGGAAAGAATCT	195
	antisense	GAGGTGCTGATGTACCAGTTGG	
Arg-1	sense	GCATATCTGCCAAAGACATCGT	139
	antisense	TCTTCCATCACCTTGCCAATC	
IL-10	sense	TACAGCCGGGAAGACAATAACT	142
	antisense	TACAGCCGGGAAGACAATAACT	

2.11. Analysis of cytokines

To determine the concentration of the proinflammatory cytokines including TNF-α, IL-6, MCP-1, IFN-γ and IL-12p70 and the anti- inflammatory cytokine IL-10 in colons, BD™ Cytometric Bead Array (CBA) Mouse Inflammation Kit (BD Biosciences, #552364, Franklin Lakes, NJ, USA) was used according to the supplier's instruction. Data were analyzed with FCAP Array software.

2.12. Flow cytometry

and dead cells were excluded with fixable live/dead stain (Fixable Viability Dye Zombie NIR, BioLegend, San Diego, California, USA). And Spleen and mesenteric lymph nodes (MLNs) single-cell suspensions then cells were fixed and permeabilized with Fix/Perm buffer (BD Biowere harvested by gently pushing cells through a 70-μm cell strainer sciences) to stain for intracellular markers. Finally, stained cells were with a syringe piston. First, cells were stained for extracellular markers analyzed by flow cytometer.

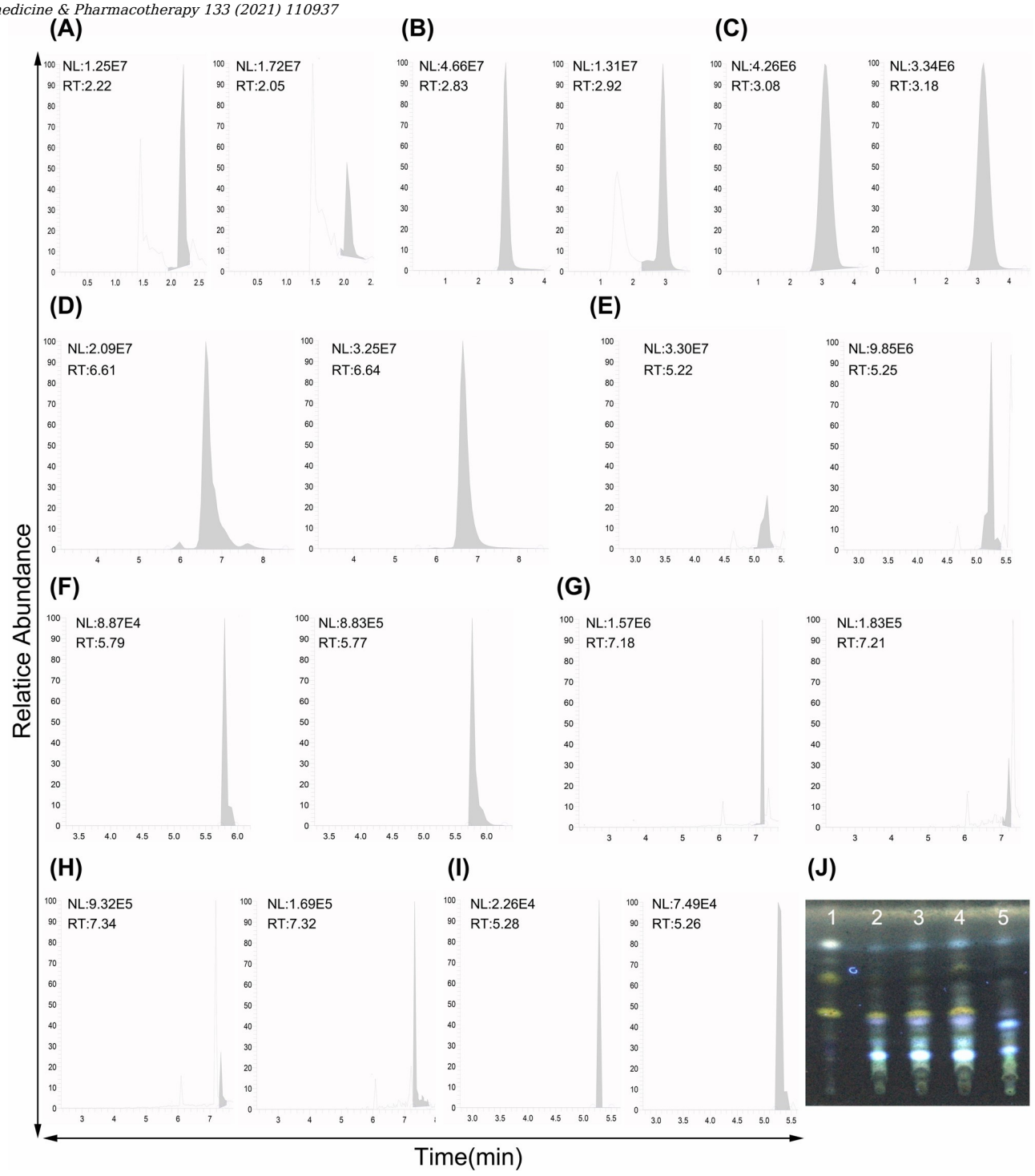

Fig. 1. Analysis of the constituents in CSD by HPLC-MS/MS and TLC method. (A) Matrine: Matrine in CSD (left panel); Matrine in standard sample (right panel). (B) Oxymatrine: Oxymatrine in CSD (left panel); Oxymatrine in standard sample (right panel). (C) Gallic acid: Gallic acid in CSD (left panel); Gallic acid in standard sample (right panel). (D) Glycyrrhizic acid: Glycyrrhizic acid in CSD (left panel); Glycyrrhizic acid in standard sample (right panel). (E) Liquiritin: Liquiritin in CSD (left panel); Liquiritin in standard sample (right panel). (F) Ginsenoside Rb1: Ginsenoside Rb1 in CSD (left panel); Ginsenoside Rb1 in standard sample (right panel). (G) Indigo: Indigo in CSD (left panel); Indigo in standard sample (right panel). (H) Indirubin: Indirubin in CSD (left panel); Indirubin in standard sample (right panel). (I) Notoginsenoside R1: Notoginsenoside R1 in CSD (left panel); Notoginsenoside R1 in standard sample (right panel). (J)The lane 1, 2 and 3 were loaded with aqueous extract of CSD; line 4 was loaded with positive sample of Bletilla striata (Thunb.) Reichb. f.; line 5 was loaded with negative sample that contained no Bletilla striata (Thunb.) Reichb. f..

2.13. Statistical analysis

Data are presented as mean ± standard deviation (SD), which were calculated by Graphpad Prism 7 (San Diego, CA). Statistical differences were determined by one-way ANOVA (for more than two groups) with Tukey's multiple comparison as a post hoc test. P values ≤ 0.05 were considered significant.

3. Results

3.1. Major components of CSD by HPLC-MS/MS and TLC method

The identification of CSD constituents was performed via HPLC-MS/ MS analysis and six components in CSD were identified based on the comparison of the retention times and peak areas with that of the standards. The representative diagram of nine active ingredients in the six herbs was depicted in Fig. 1. Matrine and Oxymatrine in CSD were illustrated in Fig. 1A and B, respectively. Gallic acid, Glycyrrhizic acid and Liquiritin in CSD were also described in Fig. 1C, D and E, everally. And Fig. 1F, G and H showed Ginsenoside Rb1, Indigo and Indirubin in turn. Likewise, Notoginsenoside R1 in CSD was detected (Fig. 1I). On TLC analysis, Bletilla striata (Thunb.) Reichb. f. in CSD was successfully separated by development on the plate (Fig. 1J). The CSD sample solution (lane 1, 2, 3) produced sepia spot, which developed at the same position as that produced by positive sample (lane 4), while spots with similar color were not observed in negative control solution (lane 5).

3.2. CSD relieves DSS-induced colitis in mice

Colitis was induced in mice through administration of 3% DSS for 7 days (Fig. 2A). During the experiment, the body weight of animals in DSS group continued to decrease significantly from day 3 (Fig. 2B). Compared with the DSS group, body weight loss dramatically improved in mice treated with CSD of medium and high dose as well as mesalazine ($p < 0.05$). Furthermore, the DAI score, assessing the severity of colitis, increased distinctly after DSS treatment, whereas it was markedly lower in the CSD and mesalazine groups (Fig. 2E). Accompanied with clinical manifestations of bloody diarrhea and body weight reduction, the colon length was apparently shorter in the DSS group in comparison with the CON group (Fig. 2C and D). And such change of colon shortening could be rescued by CSD and mesalazine therapy. In line with the above findings, epithelial crypt damage, mucosa edema, depletion of goblet cells and inflammatory cell infiltration were observed in HE staining of the DSS group, which was in sharp contrast to the normal group (Fig. 2G). Nevertheless, the CSD group exhibited obvious protection of mucosa damage and less histological inflammation, which showed a lower histopathological score (Fig. 2F). Combined, these results demonstrate that CSD exerts therapeutic effects on DSS-induced colitis. *3.3. CSD regulates cytokine expression levels in colon tissues*

Compared with the CON group, the protein levels of IL-6, IFN-γ, IL- 12p70, TNF and MCP-1 were significantly elevated in colonic tissues of mice with oral administration of DSS (Fig. 3A-E). And mRNA expression of TNF-α, MCP-1 and IL-1β also showed a similar tendency of increase in proinflammatory factors (Fig. 3G, H and J). However, the expression of IL-10, anti-inflammatory cytokine, was decreased in both protein and mRNA following the treatment of DSS. The concentration of proinflammatory cytokines mentioned above were drastically suppressed by the administration of CSD and mesalazine. Besides, CSD was able to up- regulate the level of IL-10 in the colons of mice with DSS-induced colitis. Thus, our data confirm that CSD could inhibit the overwhelming inflammatory response, partly responsible for the treatment of UC.

3.4. CSD attenuates DSS-induced damage to murine intestinal epithelial tight junction

In colonic segments obtained from normal mice, ultrastructurally, microvilli displayed normal architecture and the tight junctions (TJs), directly beneath the microvilli, was narrow and intact (Fig. 4). In contrast, there were significant alterations in TJs and microvilli ultra- structure in mice orally gavaged with DSS. TJs were profoundly altered with an increase of the paracellular space of varying degrees of saccular dilatation. Furthermore, areas with rarefaction or disappeared microvilli were observed, which were extensive and evident in DSS group. However, the damage could be improved by CSD, especially in high dose group. In murine colon sections of CSD, the microvillous structure appeared well preserved without serious distortion and effacement. TJs of mice with CSD treatment remained morphologically and functionally intact, and membranes between cells were more tightly arranged compared to DSS-induced structural changes. Mesalazine also achieved good outcomes.

To determine whether the physiological alterations in the TJ barrier were associated with changes in the distribution of TJ proteins, immunofluorescence staining was used to detect the expression of intracellular scaffolding protein ZO-1 (Fig. 5A) and transmembrane TJ protein occludin (Fig. 5B) in the colons of mice. The fluorescence intensity of ZO-1 was clearly diminished in DSS treated mice, similar to changes reported in occludin. And the redistribution and depletion of these two proteins were restored by CSD and mesalazine. No difference in the distribution or intensity of staining for ZO-1 as well as occludin was observed between CSD of high dose and mesalazine. In addition, we performed western blot on colonic tissues using specific primary antibodies for matrix metalloproteinase-9 (MMP-9), which are considered to be closely correlated with the degradation and remodeling of extracellular matrix (ECM) and regulate ECM homeostasis [10]. Immunoblot analysis manifested that increased MMP-9 caused by DSS was reduced by CSD and mesalazine (Fig. 5C and D). Together, these findings indicate that the protective effect of CSD on intestinal epithelium may be derived from its role in improving compromised tight junctions, at least partially due to suppressing dysregulated expression of MMP-9.

3.5. CSD inhibits apoptosis and promotes proliferation in colonic epithelium in mice with DSS-induced colitis

The disruption of homeostasis between proliferation and apoptosis in the colonic crypts is engaged in the pathogenesis of UC in humans [11, 12]. So, the proliferation and apoptosis of colon epithelial cells were examined by immunology technique. Cell proliferation was evaluated by Ki67 immunoreactivity and apoptosis by immunoblot

analysis. The number of Ki67 positive cells mainly limited to the lower part of the colonic crypt decreased sharply in DSS-challenged mice as compared to the normal mice, while CSD had protected mice against DSS-induced colitis accompanied with distinct increased Ki67 positive cell count (Fig. 6A). Apoptosis induction was confirmed by staining for cleaved caspase-3, a biochemical marker of apoptosis, in colonic specimens from mice subjected to colitis in comparison with the healthy mice (Fig. 6B and C). As expected, CSD administration significantly inhibited active caspase-3 expression in the inflamed intestines. And these beneficial effects also could be observed in mice treated with mesalazine. Overall, these results suggest that CSD helps maintain the intestinal epithelium barrier through not only preventing apoptosis but also enhancing proliferation.

3.6. CSD improves intestinal permeability and regulating Notch signaling pathway

To determine whether CSD can affect the mucus barrier and intestinal permeability, which are important for mucosal barrier, we firstly detected the concentration of FITC-Dextran 4000 in plasma reflecting

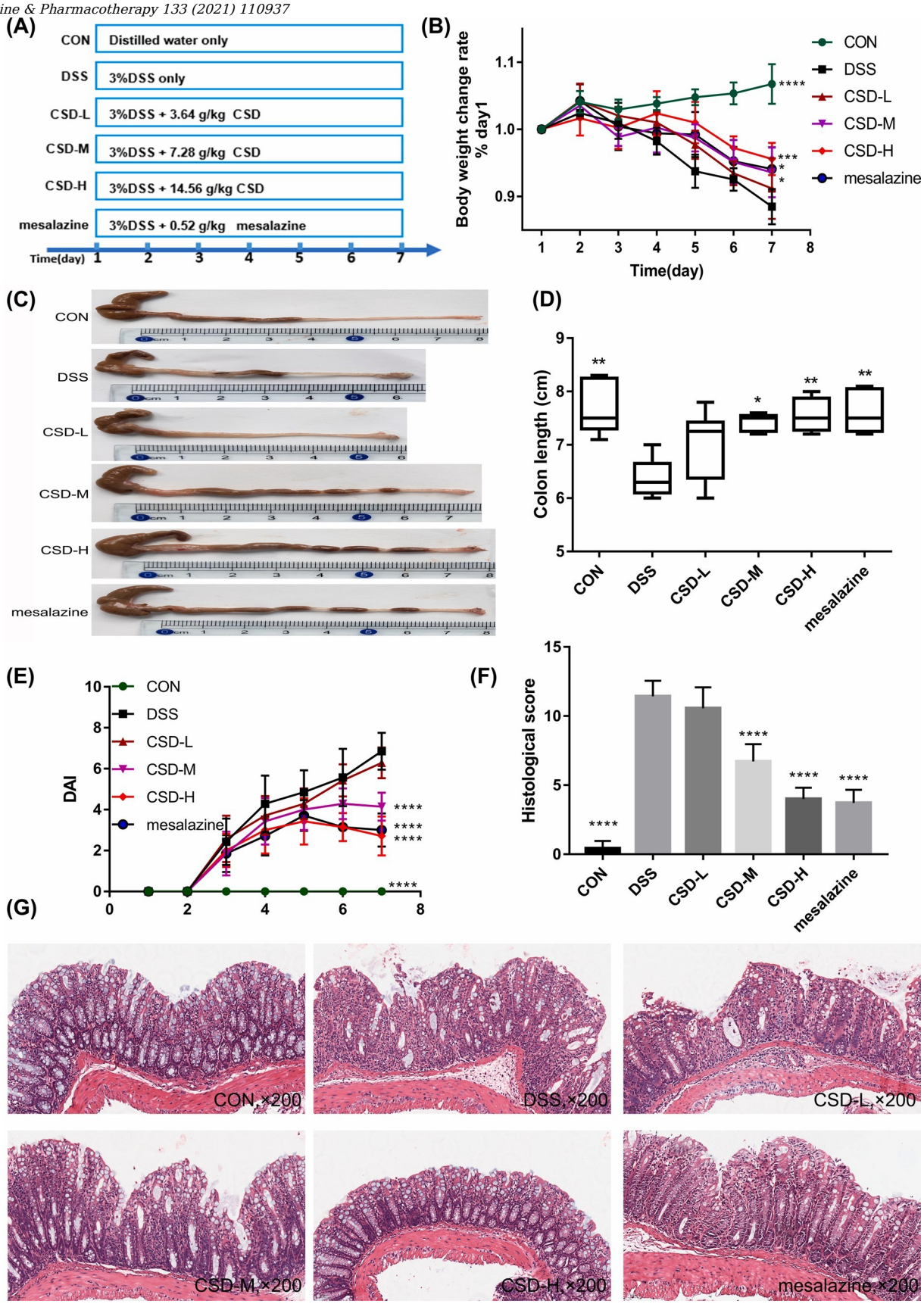

Fig. 2. CSD attenuates DSS-induced damage. (A) The schematic of UC model and drug treatment. (B) Changes of body weight. (C) Statistics of colon length. (D) Representative photograph of colons. (E) DAI score. (F) Histology score based on HE staining method. (G) HE staining (magnification ×200). Data were expressed as mean ± SD. * $p < 0.05$, ** $p < 0.01$, *** $p < 0.001$, **** $p < 0.0001$, vs. DSS group.

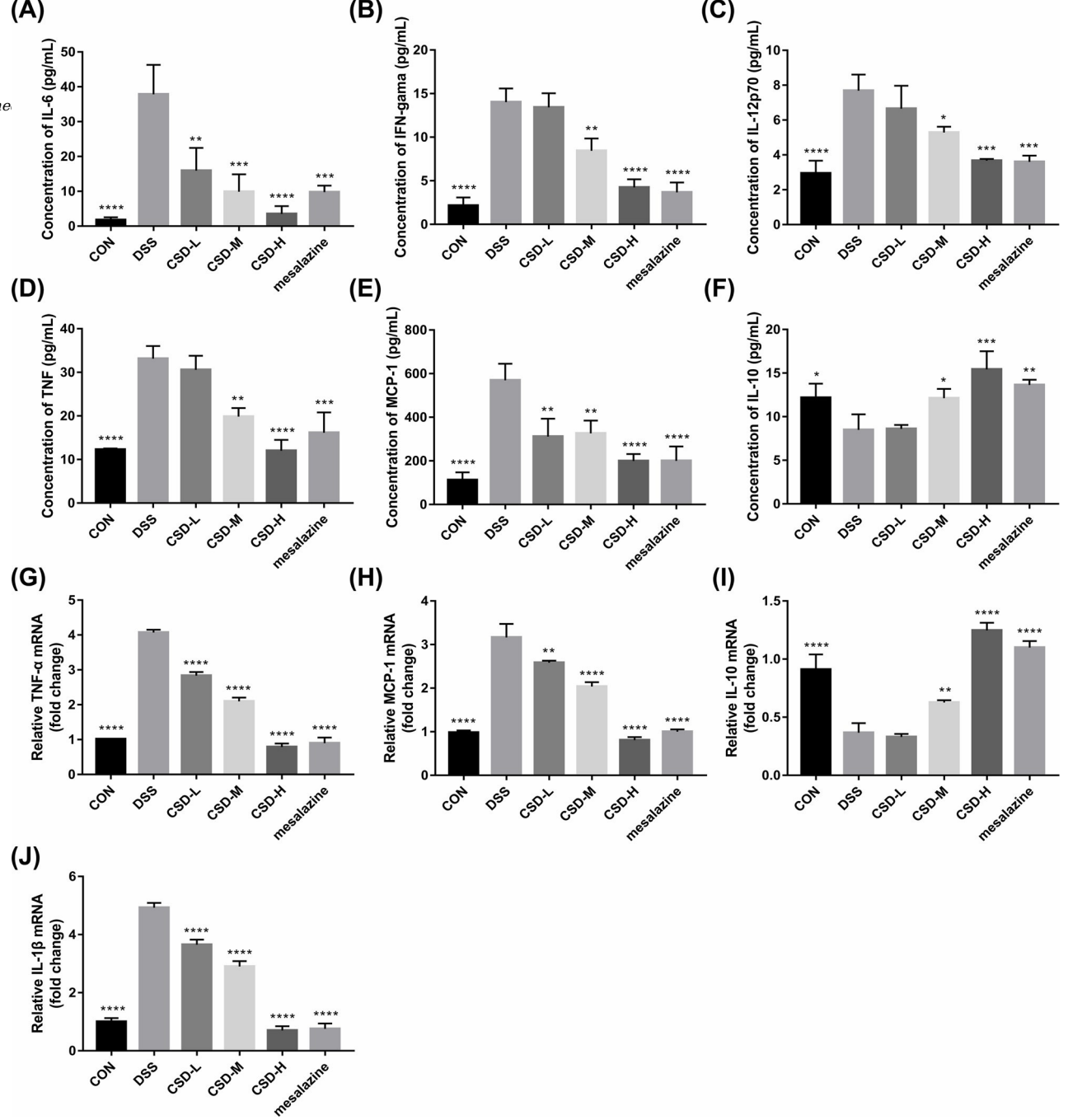

Fig. 3. CSD affects production of proinflammatory and anti-inflammatory cytokines in DSS-induced colitis mice. CBA Mouse Inflammation Kit was applied to detect the protein levels of cytokines including IL-6 (A), IFN-γ (B), IL-12p70 (C), TNF (D), MCP-1 (E), and IL-10 (F). And qRT-PCR was used to examine the mRNA expression of TNF-α (G), MCP-1 (H), IL-10 (I) and IL-1β (J). Data were expressed as mean ± SD of three independent experiments. * $p < 0.05$, ** $p < 0.01$, *** $p < 0.001$, **** $p < 0.0001$, vs. DSS group.

intestinal permeability. In DSS-challenged mice, the concentration of FITC-Dextran 4000 (2.173 ± 0.267 μg/mL) in plasma was obviously increased compared to that of the healthy controls (0.375 ± 0.101 μg/mL), almost 5.79 fold (Fig. 7G). Both high-dose CSD and mesalazine improved intestinal permeability strikingly. As shown in Fig. 7A, the serious depletion of mature goblet cells with fewer filled goblet cells and associated mucus were confirmed after DSS challenge compared with those of normal untreated mice by PAS staining. Importantly, high-dose CSD and mesalazine treatment remarkedly improved the overwhelming loss of mucus-producing goblet cells.

Through the above experiments, we have verified that CSD can promote the recovery of the defective colonic epithelial cell barrier and damaged mucus barrier of mice, consequently reducing the intestinal permeability. Therefore, we speculate that CSD may affect the proliferation and differentiation of intestinal epithelial cells (IECs) and thus regulate the secretion of mucus. In the colon, the mucus layer that covers the epithelial cells is recognized as an important ingredient in the gut protection. MUC2 mucin, the gel-forming mucin secreted by goblet cell, is the major component of mucus, which builds a mucus barrier that excludes the resident bacteria from a direct contact with the underlining epithelia to avoid overt immune responses from the adaptive and innate systems [13]. In the intestine, Notch signaling, especially Notch1, regulates stem cell-fate determination in the crypt [14]. Once stimulated, activation of Notch upon ligand binding promotes the expression of Hes-1 (Hairy and Enhancer-of-split-1), which then would suppress downstream Math1, resulting in an increase of enterocytes in parallel with restricting differentiation into goblet cells and MUC2 expression [15]. As a consequence of this, we studied the status of Notch signaling and relevant elements. As described in Fig. 7B-F, immunoblotting revealed that the protein expression of Notch1 and Hes1 was markedly increased, indicating that the Notch signaling pathway in the colon tissue was activated, while the levels of downstream ATOH1 and MUC2 decreased in colons of mice from the DSS group. After the oral administration of CSD and mesalazine, the reduction in Notch1 and Hes1 expression was found. Moreover, the ATOH1 and MUC2 expression was significantly increased compared to the DSS group. The expression trend of MUC2 in western blot analysis is consistent with that observed in PAS staining above. Taken together, these results strongly suggest that CSD improves intestinal permeability and the loss of MUC2 through blocking Notch signaling pathway.

3.7. CSD promotes phenotypic change in macrophage phenotype in colitis mice

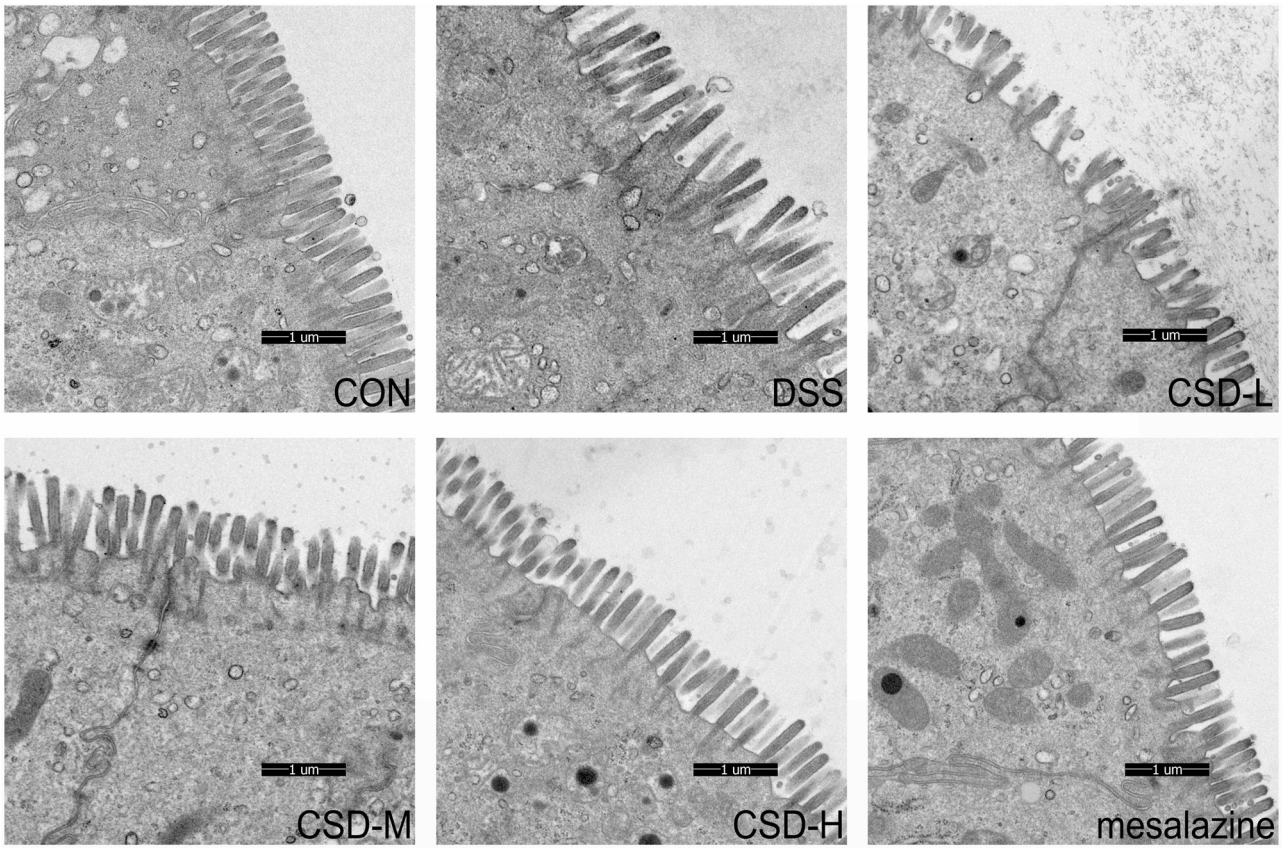

Fig. 4. Electron micrograph images of colonic segments harvested from mice with different treatment. Groups are identified as shown. Scale bar =1 μm.

To further understand the potential mechanism by which CSD therapy mitigate intestinal inflammation and improve gut barrier function, we analyzed the polarization of M1 and M2 macrophages by flow cytometry and qRT-PCR. M1 macrophages are usually considered to be pro-inflammatory while M2 macrophages are equipped with anti- inflammatory, pro-healing and regulatory properties. As shown in Fig. 8A and B, the M1/M2 macrophage ratios in spleen and mesenteric lymph nodes (MLNs) isolated from DSS-induced mice was significantly enhanced, which were 2.13-fold and 1.87-fold respectively more than that in normal untreated mice. CSD, particularly high dose, and mesalazine reduced the ratio of M1 to M2 macrophages markedly. More importantly, we found that the levels of mRNAs encoding inducible nitric oxide synthase (iNOS, M1 specific mark) were down-regulated (Fig. 8C) while M2 phenotype signature genes, Arginase 1 (Arg-1) increased (Fig. 8D) in colonic tissues after CSD and mesalazine treatment compared with mice in the

DSS group. These results show that CSD resolve inflammation of the colons and accelerate wound healing partly because of phenotypic switch of macrophages from M1 to M2, which promote recovery of injured epithelial cells.

4. Discussion

Although the mechanisms responsible for UC are yet up in the air, accumulated evidence supports that the factors proposed to cause UC may be environmental stimulus, alterations in intestinal microbiota, defected intestinal barrier and genetic susceptibility, resulting in uncontrolled immune activation residing beneath the intestinal epithelium associated with excessive mucosal inflammation [16]. Although the drugs for UC therapy clinically achieve remission to some extent, the limitations in treatment response and tolerance as well as side effects should not be ignored and therefore it is needed to find alternative or adjuvant approaches. CSD, a Chinese herb of six ingredients, has been demonstrated to be effective in clinical practice. Our previous studies have confirmed that CSD can be beneficial to the improvement of DSS-induced UC [3] and related colorectal cancer [4]. We identified ten components in this prescription by HPLC-MS/MS and TLC method, mainly including Matrine, Oxymatrine,

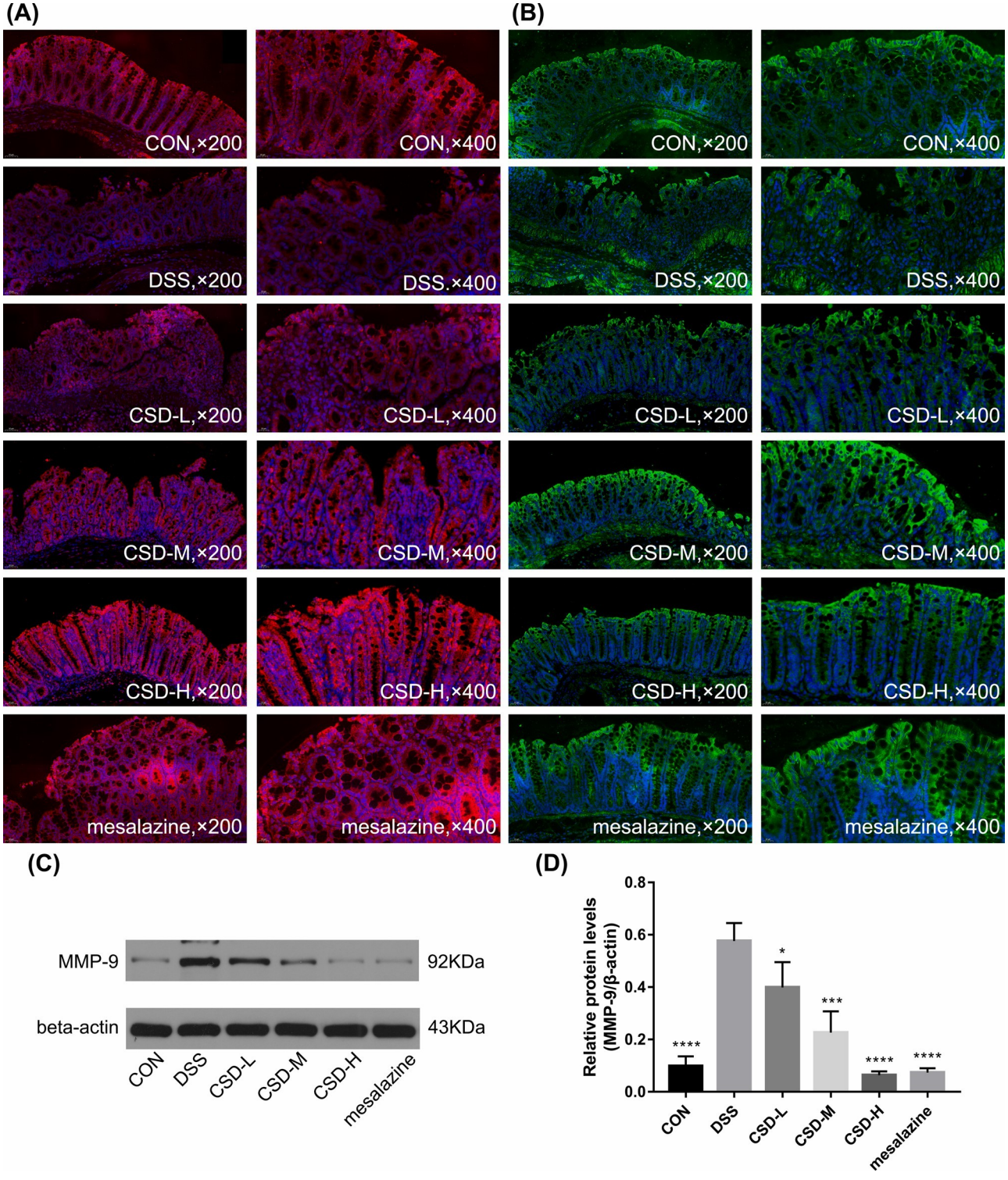

Fig. 5. CSD protects tight junctions through inhibiting expression of MMP-9 in mice after the oral administration of DSS. Merged images of immunofluorescent staining for ZO-1 (A) and occludin (B). (C) Representative western blots of MMP-9. (D) Quantitative analysis of MMP-9. Data were expressed as mean ± SD of three independent experiments. * $p < 0.05$, ** $p < 0.01$, *** $p < 0.001$, **** $p < 0.0001$, vs. DSS group.

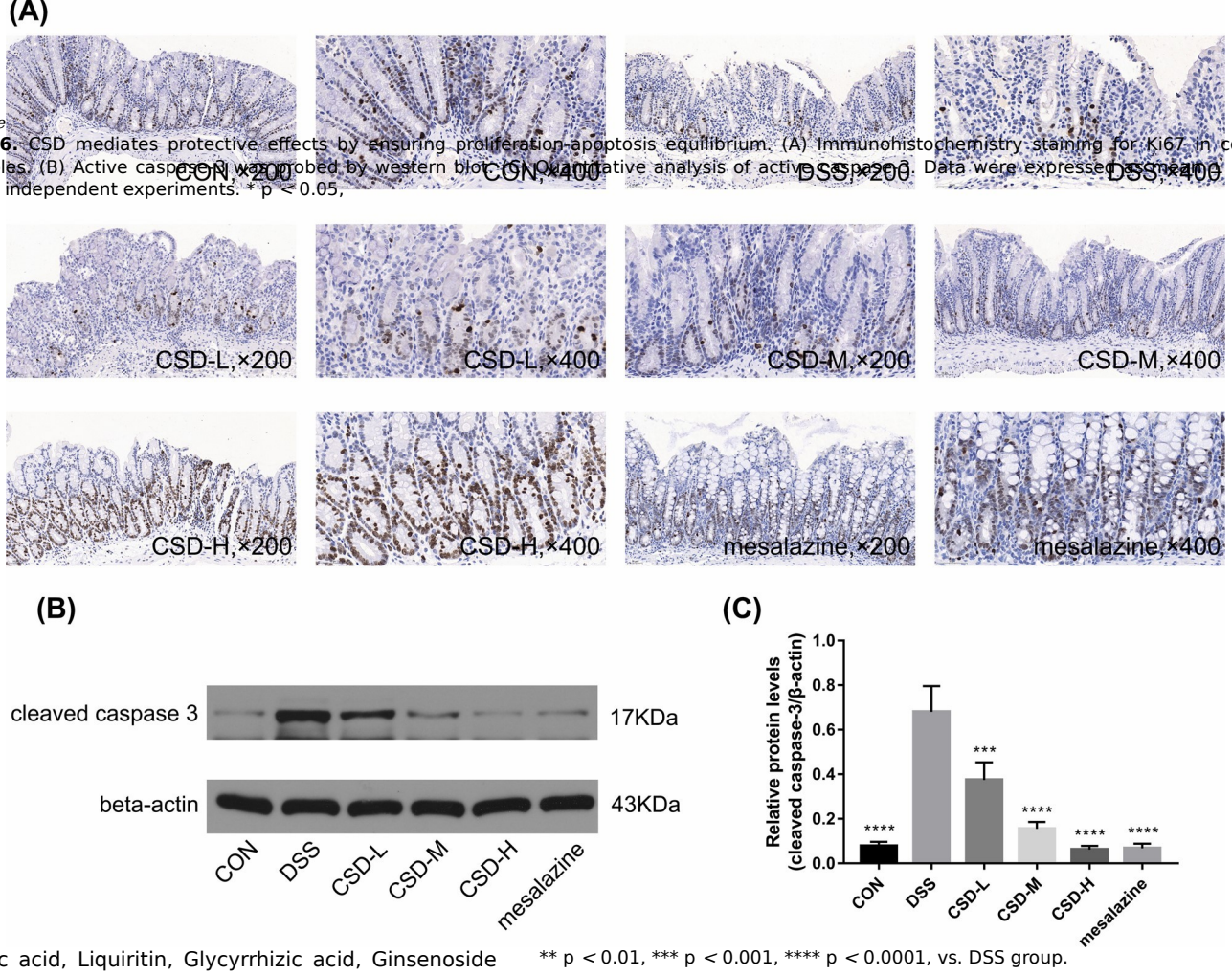

Fig. 6. CSD mediates protective effects by ensuring proliferation-apoptosis equilibrium. (A) Immunohistochemistry staining for Ki67 in colonic samples. (B) Active caspase-3 was probed by western blot. (C) Quantitative analysis of active caspase-3. Data were expressed as mean ± SD of three independent experiments. * $p < 0.05$, ** $p < 0.01$, *** $p < 0.001$, **** $p < 0.0001$, vs. DSS group.

Gallic acid, Liquiritin, Glycyrrhizic acid, Ginsenoside Rb1, Notoginsenoside R1, Indigo, Indirubin and Bletilla striata. Oxymatrine, the main effective constituent extracted from Sophora flavescens, has been proven to significantly abate DSS-induced colitis through anti-inflammatory, pro-apoptotic, down-regulating the differentiation of Th1 and Th17 cells via repressing PI3K/AKT signaling pathway [17]. Bletilla striata polysaccharide could not only promote the regeneration of intestinal mucosa, but also regulate the balance of immune system and inflammation in mice bearing UC by inhibition of TNF-α and NF-κB coupled with up-regulation of IL-10 [18]. Evidence also suggests that B. striata added to an enema showed good performance in protecting mucosa, which would form a gel on the surface of the intestinal mucosa and enhance adhesion of the preparation to the intestinal wall, therefore improving the drug concentration locally in the gut [19]. Gallic acid increased the expression of anti-inflammatory cytokines covering IL-4 and IL-10, while reduced the release of proinflammatory mediators containing IL-1, IL-6, IL-12, IL-17, IL-23, TGF-β and TNF-α via inhibiting NF-κB pathway in in culture and in vivo [20]. Moreover, indirubin administration suppressed the infiltration of CD4 + T cell and induced the formation of Foxp3-expressing regulatory T cells in the colons of mice with DSS-induced UC [21].

In this study, we found that the treatment with CSD achieved a satisfactory outcome in clinical presentations and histological changes, which was consistent with the reports of a protective effect of CSD in BALB/c mice with experimental colitis [3]. The clear improvement of weight loss, hemafecia and colon shorting were induced by CSD, particularly the high dose, as well as mesalazine used as a positive control in current experiment. Suggestive pathologic features ranging from distortion of crypt architecture to accumulation of lymphocytes and plasma cells in the lamina propria were also rescued by administration of CSD. Besides, more underlying mechanisms by which CSD protected against DSS-induced UC were revealed in present study.

The intact intestinal mucosal barriers, consisting of mechanical barrier, chemical barrier, immune barrier and biological barrier, are proposed to be pivotal for defensing the body. In inflammatory bowel disease (IBD), many of these first-line defense mechanisms are dysregulated. It appears that a disruption of the mucosal barriers in UC may exacerbate the invasion of intestinal commensal microbes and toxins, subsequently developing chronic inflammation by intensifying inappropriate immune response. IECs, composed of four lineages arising from intestinal stem cells, are a group of heterogeneous monolayer cells, and the space between neighboring epithelial cells is sealed by apical junctional complexes, which form the mechanical barrier together. Increased apoptosis, transcellular or paracellular transport all possibly

lead to alternations in epithelial barrier permeability [22]. Intestinal epithelium barrier breakdown of injury and death is recognized as a hallmark of the UC pathophysiology [23]. Compared with Crohn's disease (CD) patients and healthy people, IECs in UC patients show a higher incidence of apoptosis, and IECs in the upper part of the crypt are more prone to apoptosis than those in the lower part of the crypt [24]. Consistent with these reports, we also found that the expression of cleaved caspase-3, a well-known executioner protease of apoptosis, was increased upon DSS treatment, which exhibits several clinical and histological features similar to human UC. And, Ki67 expression appeared to be markedly lost in the colonic crypts in DSS group as well. However, these disorders were rescued by CSD, suggesting that promoting the proliferation of IECs and inhibiting its apoptosis may be one of the mechanisms of protective role of CSD in the treatment of UC.

TJs, represented by claudins, occludin, junctional adhesion molecules, and scaffold protein zonula occludins, are chiefly responsible for regulating paracellular transport and also the most principal structural component for the formation of constitutive barrier function of epithelial cells [25,26]. They function as barrier and fence under normal and pathological conditions, preventing free passage of myriad of ions and small solutes through the space between two interacting cells [25,27]. It has been demonstrated in constitutively-active myosin light chain kinase (MLCK) transgenic mice that tight junction dysfunction within intestinal epithelia leads to subclinical mucosal immune activation characterized by the recruitment or proliferation of lamina propria CD4+ lymphocytes, redistribution of CD11c + dendritic cells, elevated

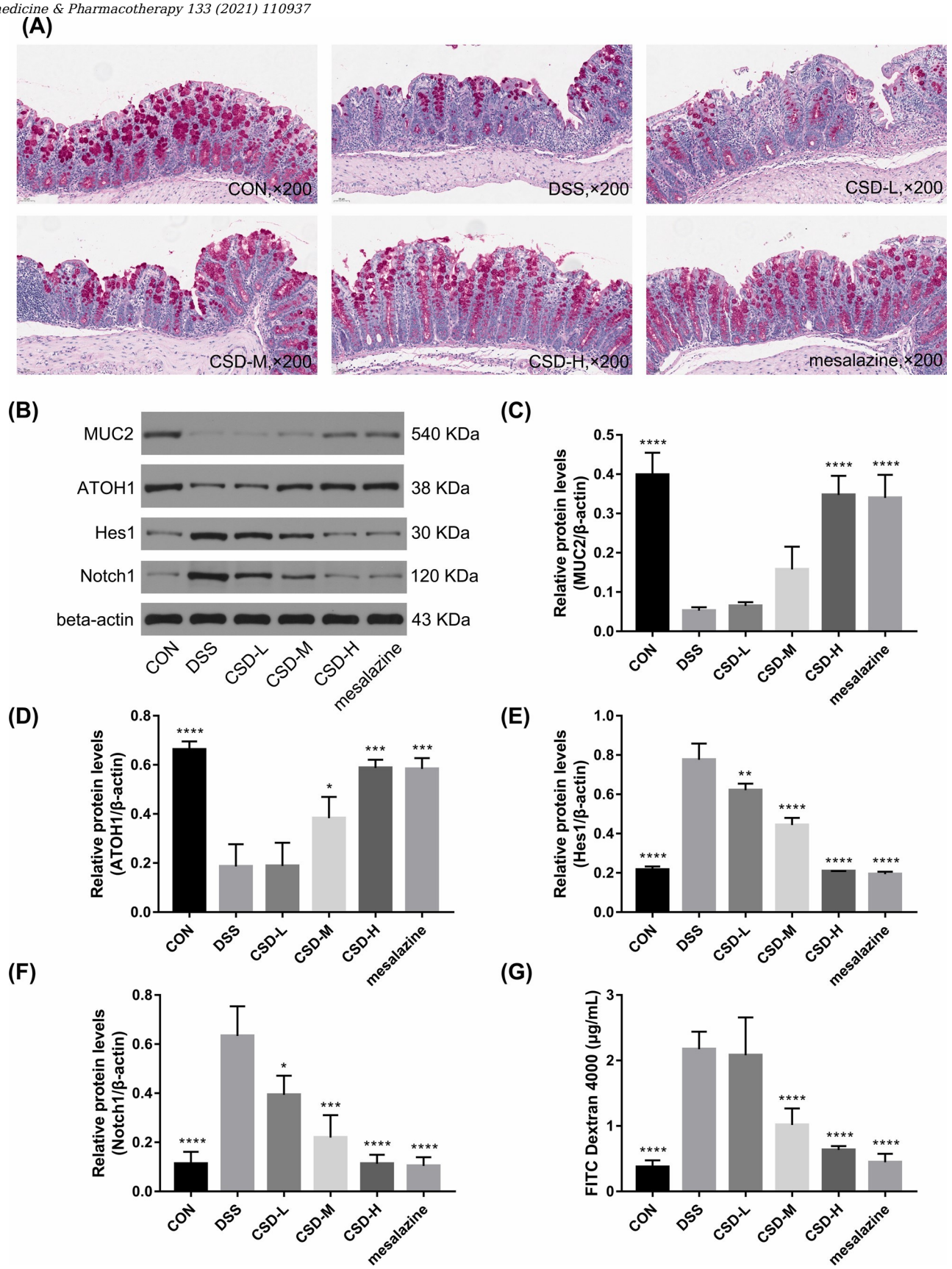

Fig. 7. CSD ameliorates DSS-induced epithelial permeability by enhancing the function of mucus layer barrier. (A) PAS staining for mucus in colonic sections. (B) Immunoblotting analysis for MUC2, ATOH1, Hes1 and Notch1 in colons of mice. Quantitative analysis of MUC2 (C), ATOH1 (D), Hes1 (E) and Notch1 (F). (G) Intestinal permeability assay. Data were expressed as mean ± SD of three independent experiments. * $p < 0.05$, ** $p < 0.01$, *** $p < 0.001$, **** $p < 0.0001$, vs. DSS group.

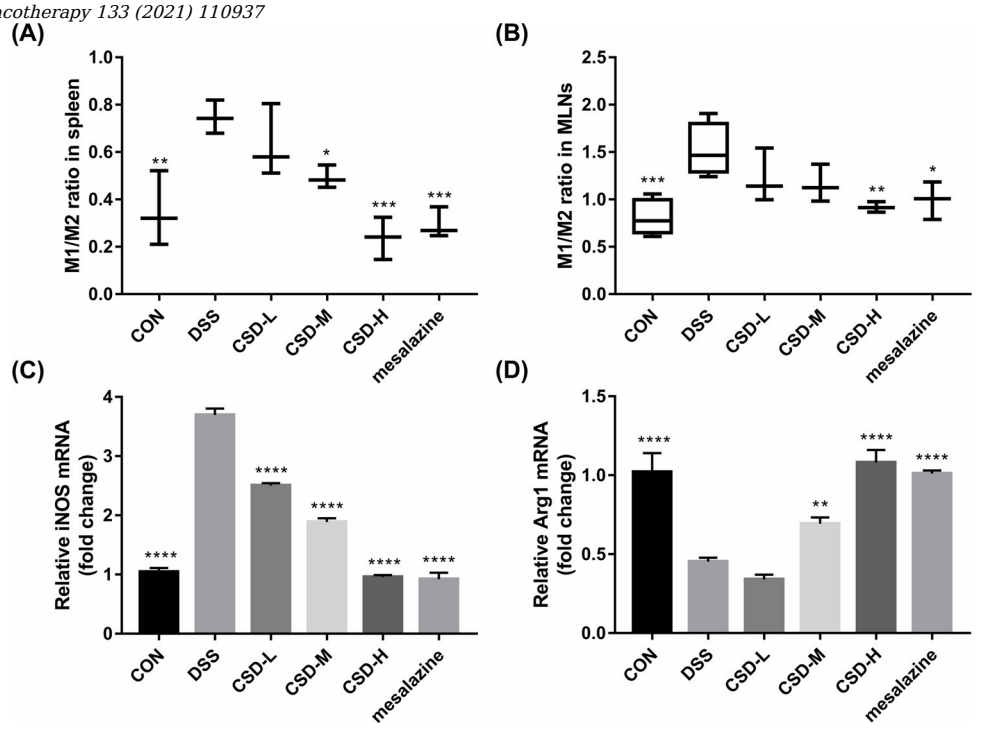

Fig. 8. Oral administration of CSD facilitates the resolution of the pro-inflammatory state of tissue macrophages. The proportion of M1 (F4/80+CD11b + CD86+) and M2 (F4/80+CD11b + CD206+) in spleen (A) and MLNs (B). And mRNAs expression of iNOS (C) and Arg-1 (D) were measured by qRT-PCR. Data were expressed as mean ± SD of three independent experiments. * $p < 0.05$, ** $p < 0.01$, *** $p < 0.001$, **** $p < 0.0001$, vs. DSS group.

mucosal transcription of IFN-γ and TNF, as well as enhanced production of epithelial MHC class I [28]. Besides, transgenic mice with this paracellular barrier defect were more susceptible to disease and displayed enhanced severity of immune-mediated colitis [28]. Similarly, data from our study revealed that the structure and distribution of TJs were disrupted combined with markedly decreased expression of ZO-1 and occluding in response to DSS, and severity of clinical presentation was far greater, while aberrant changes above were restituted in the presentation of CSD. DSS-induced proinflammatory cytokines were reported to be involved in the development of TJs loss, not only directly affecting epithelial TJ protein expression and distribution, but also acting synergistically with IFN-γ to induce MLCK and other regulatory proteins [29]. Aveleira and his colleagues discovered that TNF-α decreased the protein and mRNA content of the TJs and altered the cellular localization of these tight junction proteins, which was correlated with NF-κB and could be mitigated by a chemical inhibitor of inhibitor κB kinase (IKK) or overexpression of inhibitor κB alpha (IκBα) adenovirally thus preventing NF-κB activation [30]. Our results indicated that the Chinses herb CSD could down-regulate the level of cytokines, such as TNF-a and IL-1β. What's more, our laboratory has previously demonstrated that the expression of phospho-NF-κB p65 was reduced by CSD [3]. Therefore, we speculate that the down-regulation of NF-κBp65 phosphorylation level and downstream inflammatory mediators may be one of the mechanisms of the action of CSD against DSS-induced TJs breakdown. MMP-9 is the main metalloproteinase engaged in the development and progression of IBD [31]. MMP-9 is highly elevated in the intestine of patients with IBD, and similar results were obtained in intestinal tissue from DSS-treated mice [32]. That was also verified in our western blot results. MMP-9 could modulate the construction and function of TJ proteins and induce increase in intestinal permeability via upregulation of MLCK expression in response to inflammatory stimuli [33]. There is also evidence suggesting that MMP-9 may aggravate intestinal inflammation and cause IECs breach in UC mice [34]. Herein, we showed that CSD inhibit the release of MMP-9, exerting a protective effect on TJs and IECs.

The stratified mucus layer is another essential part of intestinal mucosal barrier, acting as the primary gate keeper for the gut protection. Mucus is produced by the goblet cells and typically contains several major components. One of these, the mucins, gives the mucus its gel-like properties. Mucus have a two-layered system with an inner and an outer mucus layer in colon. The inner mucus layer is firmly attached to the epithelium and impenetrable to colonic bacteria, while the outer is soluble and loose, generating the preferred habitat for the commensal microbes [35]. The main mucus component in the intestine is MUC2 mucin [36]. In vivo studies on genetically engineered mice by Van and others using a chemically induced DSS colitis model revealed that MUC2 deficiency in the intestine and therefore breaches in the epithelial barrier contributed to the onset and perpetuation of colitis spontaneously [37]. In DSS-induced colitis mice and patients with active UC, reduced number of goblet cells and thinner mucus layer with compromised quality were found, which allowed bacteria to penetrate and reach the epithelium and consequently led to intestinal inflammation [38,39]. Therefore, the restoration of the thickness and properties of the mucus layer as well as the number of goblet cells may be an effective method to treat UC. The published literature report that the

evolutionary conserved Notch signaling pathway mediates cell fate decisions and patterning; Notch1 and Hes1 are specifically expressed in intestinal crypts; and further mutational analysis of Hes1 and Math1, the Notch targets and downstream effectors, have indicated a requirement for Notch signaling in the regulation of intestinal epithelium development and homeostasis [40]. Canonical Notch signaling induces transcriptional activation of Hes1 by binding Notch1 intracellular domain (NICD) to RBP-Jk, and Hes1 directly binds to the 5′ promoter region of transcription factor Atoh1, leading to the decrease of Atoh1 expression and suppression of the phenotypic gene expression for secretory lineages, such as goblet cells [15]. As a result, the expression of the MUC2 was also decreased [15]. The present study also found that MUC2 protein levels decreased after DSS administration in the colonic tissues but increased substantially after treatment with CSD and mesalazine. In view of the effect of Notch singling on mucus and goblet cell, we then examined related molecules and observed that Notch signaling was abnormally activated in the DSS group, which is consistent with previous reports. Our results signify that CSD probably protect against the loss of muc-2/ goblet cell to strengthen mucus barrier via inhibiting Notch signaling.

Massive inflammatory infiltration confined to the mucosa and submucosa of the colon and rectum is one of the typical pathological manifestations of UC. The inflammatory infiltrate consists of neutrophils, lymphocytes and macrophages that penetrate the gut barrier and result in ulceration and crypt abscessation [41]. Macrophages are a heterogeneous and plastic cell population. In different stages of UC development, macrophages can show different phenotypes due to dynamic structure of the niche and exert different functions [42]. Macrophages, dependent upon their phenotype, are important effector cells of both the initiation/maintenance of inflammatory response and the resolution/regeneration processes. M2-like macrophages are believed to be regulatory, anti-inflammatory and pro-healing in an inducible rodent model of UC [43]. Accordingly, we speculated whether a timely shift in macrophage phenotype toward M2 predominance was conducive to mucosal repair. The findings of our experiment uncovered that the expression of proinflammatory cytokine profile known to be associated with M1 was decreased in the CSD group. Moreover, the M1/M2 ratio of the CSD group decreased, and the expression levels of iNOS and Arg1 decreased and increased respectively. A sharp reduction in histological signs of UC was induced by CSD intake as shown in HE staining. Combined, our observations suggest that CSD treatment could facilitate the resolution of the pro-inflammatory state of tissue macrophages and accelerate mucosal healing, thus promoting functional improvement of colonic epithelial barrier function.

5. Conclusion

In summary, the present study demonstrated that CSD displayed multifaceted protective effects against DSS-induced colitis in mice through abating intestinal inflammation, and restoring colonic barrier function via the modulation of notch signaling pathway partly.

Author contributions

HF and QC designed the experiments. HW, SC and CT performed the experiments. WW and XL analyzed the data. HW wrote the manuscript. FZ, YL, SD, TY, YD, FG, HH and XL contributed reagents/materials/ analysis tools.

Declaration of Competing Interest

The authors declare no conflict of interest.

Acknowledgement

This work was supported by the National Natural Science Foundation of China (Nos. 81774093).

References

[1] J.C. Lin, J.Q. Wu, F. Wang, F.Y. Tang, J. Sun, B. Xu, M. Jiang, Y. Chu, D. Chen, X. Li, S. Su, Y. Zhang, N. Wu, S. Yang, K. Wu, J. Liang, QingBai decoction regulates intestinal permeability of dextran sulphate sodium-induced colitis through the modulation of notch and NF-kappaB signalling, Cell Prolif. https://doi.org/52 (2019)e12547.10.1111/cpr.12547.

[2] G. Song, C. Fiocchi, J.P. Achkar, Acupuncture in inflammatory bowel disease, Inflamm. Bowel Dis. 25 (2019) 1129–1139, https://doi.org/10.1093/ibd/izy371. [3] M. Xu, X.Y. Duan, Q.Y. Chen, H. Fan, Z.C. Hong, S.J. Deng, Z. Nan, H. Wu, Y. L. Dong, Y.J. Liu, C.Z. Zhou, Effect of compound sophorae decoction on dextran sodium sulfate (DSS)-induced colitis in mice by regulating Th17/Treg cell balance, Biomed. Pharmacother. 109 (2019) 2396–2408, https://doi.org/10.1016/j. biopha.2018.11.087.

[4] S. Deng, Q. Tang, X. Duan, H. Fan, L. Zhang, X. Zhu, J. Hu, M. Xu, Q. Chen, Y. Liu, Y. Dong, Z. Nan, H. Wu, Uncovering the anticancer mechanism of compound sophorae decoction against ulcerative colitis-related colorectal Cancer in mice, Evid.-based Complement Altern. Med. 2019 (2019), 8128170, https://doi.org/ 10.1155/2019/8128170.

[5] A. Michielan, R. D'inca, Intestinal permeability in inflammatory bowel disease: pathogenesis, clinical evaluation, and therapy of leaky gut, Mediat. Inflamm. 2015 (2015), 628157, https://doi.org/10.1155/2015/628157.

[6] D. Rachmilewitz, F. Karmeli, K. Takabayashi, T. Hayashi, L. Leider-Trejo, J. Lee, L. M. Leoni, E. Raz, Immunostimulatory DNA ameliorates experimental and spontaneous murine colitis, Gastroenterology 122 (2002) 1428–1441, https://doi.org/10.1053/gast.2002.32994.

[7] K. Munakata, M. Koi, T. Kitajima, S. Tseng-Rogenski, M. Uemura, H. Matsuno, K. Kawai, Y. Sekido, T. Mizushima, Y. Toiyama, T. Yamada, M. Mano, E. Mita, M. Kusunoki, M. Mori, J.M. Carethers, Inflammation-associated microsatellite alterations caused by MSH3 dysfunction are prevalent in ulcerative colitis and increase with neoplastic advancement, Clin. Transl. Gastroenterol. 10 (2019), e00105, https://doi.org/10.14309/ctg.0000000000000105.

[8] M. Pervin, M.A. Hasnat, J.H. Lim, Y.M. Lee, E.O. Kim, B.H. Um, B.O. Lim, Preventive and therapeutic effects of blueberry (Vaccinium corymbosum) extract against DSS-induced ulcerative colitis by regulation of antioxidant and inflammatory mediators, J. Nutr. Biochem. 28 (2016) 103–113, https://doi.org/ 10.1016/j.jnutbio.2015.10.006.

[9] V. Volynets, A. Reichold, G. Bardos, A. Rings, A. Bleich, S.C. Bischoff, Assessment of the intestinal barrier with five different permeability tests in healthy C57BL/6J and BALB/cJ mice, Dig. Dis. Sci. 61 (2016) 737–746, https://doi.org/10.1007/ s10620-015-3935-y.

[10] J.D. Mott, Z. Werb, Regulation of matrix biology by matrix metalloproteinases, Curr. Opin. Cell Biol. 16 (2004) 558–564, https://doi.org/10.1016/j. ceb.2004.07.010.

[11] B.A. Jones, G.J. Gores, Physiology and pathophysiology of apoptosis in epithelial cells of the liver, pancreas, and intestine, Am. J. Physiol. 273 (1997) G1174–1188, https://doi.org/10.1152/ajpgi.1997.273.6.G1174.

[12] A.J. Watson, D.M. Pritchard, Lessons from genetically engineered animal models. VII. Apoptosis in intestinal

epithelium: lessons from transgenic and knockout mice, Am. J. Physiol.-Gastroint. Liver Physiol. 278 (2000) G1–5, https://doi.org/ 10.1152/ajpgi.2000.278.1.G1.
[13] M.E. Johansson, M. Phillipson, J. Petersson, A. Velcich, L. Holm, G.C. Hansson, The inner of the two Muc2 mucin-dependent mucus layers in colon is devoid of bacteria, Proc. Natl. Acad. Sci. U. S. A. 105 (2008) 15064–15069, https://doi.org/ 10.1073/pnas.0803124105.
[14] C. Blanpain, V. Horsley, E. Fuchs, Epithelial stem cells: turning over new leaves, Cell 128 (2007) 445–458, https://doi.org/10.1016/j.cell.2007.01.014.
[15] X. Zheng, K. Tsuchiya, R. Okamoto, M. Iwasaki, Y. Kano, N. Sakamoto, T. Nakamura, M. Watanabe, Suppression of hath1 gene expression directly regulated by hes1 via notch signaling is associated with goblet cell depletion in ulcerative colitis, Inflamm. Bowel Dis. 17 (2011) 2251–2260, https://doi.org/ 10.1002/ibd.21611.
[16] G.P. Ramos, K.A. Papadakis, Mechanisms of disease: inflammatory bowel diseases, Mayo Clin. Proc. 94 (2019) 155–165, https://doi.org/10.1016/j.mayocp.2018.09.013.
[17] Q. Chen, X. Duan, H. Fan, M. Xu, Q. Tang, L. Zhang, Z. Shou, X. Liu, D. Zuo, J. Yang, S. Deng, Y. Dong, H. Wu, Y. Liu, Z. Nan, Oxymatrine protects against DSS- induced colitis via inhibiting the PI3K/AKT signaling pathway, Int. Immunopharmacol. 53 (2017) 149–157, https://doi.org/10.1016/j.intimp.2017.10.025.
[18] C.Y. Ke, C.J. Zhao, Effects of Bletilla striata polysaccharides on ulcerative colitis, J. Chinese Pharm. Sci. 22 (2011) 2132–2134, https://doi.org/10.1007/s10008- 010-1224-4.
[19] D. Xu, Y. Pan, J. Chen, Chemical constituents, pharmacologic properties, and clinical applications of bletilla striata, Front. Pharmacol. 10 (2019) 1168, https://doi.org/10.3389/fphar.2019.01168.
[20] L. Zhu, P. Gu, H. Shen, Gallic acid improved inflammation via NF-kappaB pathway in TNBS-induced ulcerative colitis, Int. Immunopharmacol. 67 (2019) 129–137, https://doi.org/10.1016/j.intimp.2018.11.049.
[21] W. Gao, Y. Guo, C. Wang, Y. Lin, L. Yu, T. Sheng, Z. Wu, Y. Gong, Indirubin ameliorates dextran sulfate sodium-induced ulcerative colitis in mice through the inhibition of inflammation and the induction of Foxp3-expressing regulatory T cells, Acta Histochem. 118 (2016) 606–614, https://doi.org/10.1016/j.acthis.2016.06.004.
[22] M. Camilleri, Leaky gut: mechanisms, measurement and clinical implications in humans, Gut 68 (2019) 1516–1526, https://doi.org/10.1136/gutjnl-2019-318427. [23] R. Garcia-Carbonell, J. Wong, J.Y. Kim, L.A. Close, B.S. Boland, T.L. Wong, P. A. Harris, S.B. Ho, S. Das, P.B. Ernst, R. Sasik, W.J. Sandborn, J. Bertin, P.J. Gough, J.T. Chang, M. Kelliher, D. Boone, M. Guma, M. Karin, Elevated A20 promotes TNF-induced and RIPK1-dependent intestinal epithelial cell death, Proc. Natl. Acad. Sci. U. S. A. 115 (2018) E9192–e9200, https://doi.org/10.1073/ pnas.1810584115.
[24] H.S. Souza, C.J. Tortori, M.T. Castelo-Branco, A.T. Carvalho, V.S. Margallo, C.
F. Delgado, I. Dines, C.C. Elia, Apoptosis in the intestinal mucosa of patients with inflammatory bowel disease: evidence of altered expression of FasL and perforin cytotoxic pathways, Int. J. Colorectal Dis. 20 (2005) 277–286, https://doi.org/ 10.1007/s00384-004-0639-8.
[25] T. Oshima, H. Miwa, Gastrointestinal mucosal barrier function and diseases, J. Gastroenterol. 51 (2016) 768–778, https://doi.org/10.1007/s00535-016-1207- z.
[26] A. Fasano, Zonulin and its regulation of intestinal barrier function: the biological door to inflammation, autoimmunity, and cancer, Physiol. Rev. 91 (2011) 151–175, https://doi.org/10.1152/physrev.00003.2008.
[27] R. Ahmad, M.F. Sorrell, S.K. Batra, P. Dhawan, A.B. Singh, Gut permeability and mucosal inflammation: bad, good or context dependent, Mucosal Immunol. 10 (2017) 307–317, https://doi.org/10.1038/mi.2016.128.
[28] L. Su, L. Shen, D.R. Clayburgh, S.C. Nalle, E.A. Sullivan, J.B. Meddings, C. Abraham, J.R. Turner, Targeted epithelial tight junction dysfunction causes immune activation and contributes to development of experimental colitis, Gastroenterology 136 (2009) 551–563, https://doi.org/10.1053/j.gastro.2008.10.081.
[29] M. Amasheh, I. Grotjohann, S. Amasheh, A. Fromm, J.D. Soderholm, M. Zeitz, M. Fromm, J.D. Schulzke, Regulation of mucosal structure and barrier function in rat colon exposed to tumor necrosis factor alpha and interferon gamma in vitro: a novel model for studying the pathomechanisms of inflammatory bowel disease cytokines, Scand. J. Gastroenterol. 44 (2009) 1226–1235, https://doi.org/10.1080/00365520903131973.
[30] C.A. Aveleira, C.M. Lin, S.F. Abcouwer, A.F. Ambrosio, D.A. Antonetti, TNF-alpha signals through PKCzeta/NF-kappaB to alter the tight junction complex and increase retinal endothelial cell permeability, Diabetes 59 (2010) 2872–2882, https://doi.org/10.2337/db09-1606.
[31] R. Al-Sadi, M. Youssef, M. Rawat, S. Guo, K. Dokladny, M. Haque, M.D. Watterson, T.Y. Ma, MMP-9-induced increase in intestinal epithelial tight permeability is mediated by p38 kinase signaling pathway activation of MLCK gene, Am. J. Physiol.-Gastroint. Liver Physiol. 316 (2019) G278–g290, https://doi.org/ 10.1152/ajpgi.00126.2018.
[32] P.J. Koelink, S.A. Overbeek, S. Braber, M.E. Morgan, P.A. Henricks, M. Abdul Roda, H.W. Verspaget, S.C. Wolfkamp, A.A. Te Velde, C.W. Jones, P.L. Jackson, J.
E. Blalock, R.W. Sparidans, J.A. Kruijtzer, J. Garssen, G. Folkerts, A.D. Kraneveld, Collagen degradation and neutrophilic infiltration: a vicious circle in inflammatory bowel disease, Gut 63 (2014) 578–587, https://doi.org/10.1136/gutjnl-2012- 303252.
[33] P. Nighot, R. Al-Sadi, M. Rawat, S. Guo, D.M. Watterson, T. Ma, Matrix metalloproteinase 9-induced increase in intestinal epithelial tight junction permeability contributes to the severity of experimental DSS colitis, Am. J. Physiol.-Gastroint. Liver Physiol. 309 (2015) G988–997, https://doi.org/10.1152/ ajpgi.00256.2015.
[34] H. Liu, N.R. Patel, L. Walter, S. Ingersoll, S.V. Sitaraman, P. Garg, Constitutive expression of MMP9 in intestinal epithelium worsens murine acute colitis and is associated with increased levels of proinflammatory cytokine Kc, Am. J. Physiol.- Gastroint. Liver Physiol. 304 (2013) G793–803, https://doi.org/10.1152/ ajpgi.00249.2012.
[35] T. Pelaseyed, J.H. Bergstrom, J.K. Gustafsson, A. Ermund, G.M. Birchenough, A. Schutte, S. Van Der Post, F. Svensson, A.M. Rodriguez-Pineiro, E.E. Nystrom, C. Wising, M.E. Johansson, G.C. Hansson, The mucus and mucins of the goblet cells and enterocytes provide the first defense line of the gastrointestinal tract and interact with the immune system, Immunol. Rev. 260 (2014) 8–20, https://doi.org/10.1111/imr.12182.
[36] G.C. Hansson, M.E. Johansson, The inner of the two Muc2 mucin-dependent mucus layers in colon is devoid of bacteria, Gut Microbes 1 (2010) 51–54, https://doi.org/10.4161/gmic.1.1.10470.
[37] M. Van Der Sluis, B.A. De Koning, A.C. De Bruijn, A. Velcich, J.P. Meijerink, J. B. Van Goudoever, H.A. Buller, J. Dekker, I. Van Seuningen, I.B. Renes, A.
W. Einerhand, Muc2-deficient mice spontaneously develop colitis, indicating that MUC2 is critical for colonic protection, Gastroenterology 131 (2006) 117–129, https://doi.org/10.1053/j.gastro.2006.04.020.
[38] M.E. Johansson, J.K. Gustafsson, J. Holmen-Larsson, K.S. Jabbar, L. Xia, H. Xu, F. K. Ghishan, F.A. Carvalho, A.T. Gewirtz, H. Sjovall, G.C. Hansson, Bacteria penetrate the normally impenetrable inner colon mucus layer in both murine colitis models and patients with ulcerative colitis, Gut 63 (2014) 281–291, https:// doi.org/10.1136/gutjnl-2012-303207.
[39] M. Shinoda, M. Shin-Ya, Y. Naito, T. Kishida, R. Ito, N. Suzuki, H. Yasuda, J. Sakagami, J. Imanishi, K. Kataoka, O. Mazda, T. Yoshikawa, Early-stage blocking of Notch signaling inhibits the depletion of goblet cells in dextran sodium sulfate-induced colitis in mice, J. Gastroenterol. 45 (2010) 608–617, https://doi.org/ 10.1007/s00535-010-0210-z.
[40] N. Schroder, A. Gossler, Expression of Notch pathway components in fetal and adult mouse small intestine, Gene Expr. Patterns 2 (2002) 247–250, https://doi.org/10.1016/s1567-133x(02)00060-1.
[41] M. Cottone, D. Scimeca, F. Mocciaro, G. Civitavecchia, G. Perricone, A. Orlando, Clinical course of ulcerative colitis, Dig. Liver Dis. 40 (Suppl 2) (2008) S247–252, https://doi.org/10.1016/s1590-8658(08)60533-2.
[42] S.L. Pull, J.M. Doherty, J.C. Mills, J.I. Gordon, T.S. Stappenbeck, Activated macrophages are an adaptive element of the colonic epithelial progenitor niche necessary for regenerative responses to injury, Proc. Natl. Acad. Sci. U. S. A. 102 (2005) 99–104, https://doi.org/10.1073/pnas.0405979102.
[43] T.J. Keane, J. Dziki, E. Sobieski, A. Smoulder, A. Castleton, N. Turner, L.J. White, S. F. Badylak, Restoring mucosal barrier function and modifying macrophage phenotype with an extracellular matrix hydrogel: potential therapy for ulcerative colitis, J. Crohns Colitis 11 (2017) 360–368, https://doi.org/10.1093/ecco-jcc/ jjw149.